比較三種離岸風場發電量預估之計算方法
Comparative Three Computational Approaches to Evaluate Energy Production of Offshore Wind Farm

范秉天 [1*]、林宗岳 [1]、陳振雄 [2]、何鎮平 [3]
財團法人中國驗船中心研究處研發組 [1]
經濟部標準檢驗局電氣檢驗科 [2]、財團法人金屬工業研究中心光機電檢測組 [3]

Bryan Nelson [1*], Tsung-Yueh Lin [1], Chen-Hsiung Chen [2], Chen-Ping Ho [3]
[1] R/D Section, Research Department, CR Classification Society
[2] Electrical Engineer Section, Bureau of Standards, Metrology & Inspection, M.O.E.A.
[3] Opt-Mechatronic Testing Section, Metal Industries Research & Development Centre
[*] Email: bnelson@crclass.org

摘要

綠色能源受到無法控制的環境因素影響，因此有效掌握發電不穩定性以達到商業風場永續經營一直是風場開發商在規劃初期重視的項目之一。然而對於大規模離岸風機陣列而言，環境變因加上與風機之間的互制效應使問題極為複雜，工程實務上多數採用數值分析方法進行風場發電容量評估。本研究探討常用的三種風機模擬數值模型：Jensen’s 模型、致動盤模型、完全風機模型等三者之異同。風機模型搭配不同背景風場的統御方程，線性化 IBZ 或 RANS 模型，可模擬整體風機陣列之氣動力現象。前者由大氣動力學發展而來，如 WAsP 軟體；後者由流體力學發展而來，商業軟體如 Star-CCM+ 等；兩者皆有數十年理論發展歷程。然本研究特別針對近年發展的風機致動盤模型搭配 RANS 的應用說明，風機陣列編制參數對整體年發電量(AEP)的影響，並以單機與陣列演示此模型於離岸風場模擬之適用性。

關鍵詞：離岸風場、跡流效應、風能評估、數值模擬。

Abstract

Due to the erraticity of wind energy conversion, wind farm developers have long emphasized the effective regulation of fluctuating power output in order to achieve sustainable operation. However, for large-scale offshore wind turbine arrays, such instability problems are further complicated by wake interaction effects. In practice, wind farm power generation capacity is typically assessed by employing numerical models. In this study, we investigate three numerical tools commonly used for wind turbine analysis, namely: Jensen's wake model, actuator disk models, and Navier-Stokes solvers. These wind turbine models are combined with different mesoscale wind field models, such as the linearized IBZ flow model and RANS models, to simulate the aerodynamic characteristics of the total wind turbine array; the former has its roots in atmospheric dynamics, and is employed by the WAsP software, while the latter has its roots in fluid mechanics, and is adopted by commercial software such as Star-CCM+; both of which have decades of theoretical development. This study, however, is particularly concerned with the coupling of the wind turbine actuator disk model with a mesoscale RANS model, an approach which has been hotly developed in recent years, to determine the effects of the wind turbine array layout parameters on the total Annual Energy Production (AEP), and to demonstrate the applicability of this model to a full offshore wind turbine array.

Keywords: offshore wind farm, wake effect, energy production, numerical simulation.

I. Introduction

Taiwan has recently started to evaluate the potential for offshore wind energy production off its west coast, which is listed by 4C Offshore Limited as one of the world's best wind locations [1], with the top 44 sites in their Global Offshore Wind Speed Rankings all located in the Taiwan Strait. Little wonder that the Taiwanese Ministry of Economic Affairs (MOEA) aims to invest a total of NT$684 billion (US$22.6 billion) to raise wind energy capacity to 4.2 GW by 2025, with 3 GW of that coming from offshore wind farms [2].

One of the more obvious challenges faced by Taiwan’s wind farms are the extreme loads exerted on the wind farm units’ structures during typhoons [3, 4], which strike the island, on average, four times every year [5]. Furthermore, the authors previously showed [6] that fatigue damage due to Taiwan’s excellent wind resources can be just as significant a challenge. This previous study considered the environmental loads exerted on a single wind farm unit during its 20 year design life, and highlighted the sensitivity of the fatigue life to the degree of fluctuation (standard deviation) of the wind loads, as well as the importance of appropriately orienting the jacket foundations according to prevailing wind and wave conditions. This previous study did not, however, consider the exacerbated fatigue loading caused by unsteady wind farm wake effects, such as wake shadowing and wake meandering (as illustrated in Figure 1) [7]. In addition to increased load fluctuations, these wake effects are also responsible for significantly reduced power production.

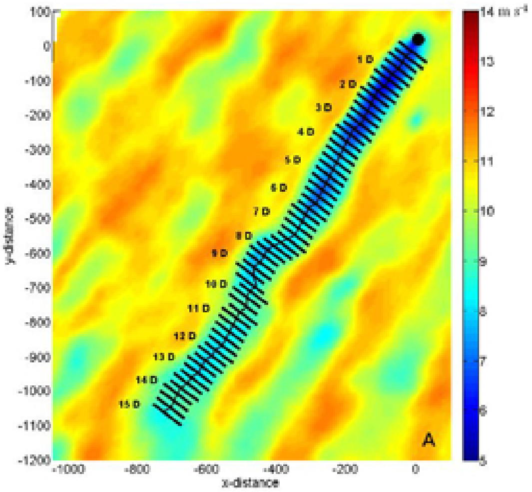

Figure 1. Wake meandering in a wind farm [7]

These turbine-turbine interactions would certainly be prevalent in the MOEA's "Thousand Wind Turbines" project, which is the motivation behind the design and implementation of the present study, namely to investigate three different numerical tools of varying degrees of fidelity which are commonly used to assess such effects.

The target wind turbine specifications and wind turbine array layout and conditions are defined in the second section of this paper, while the three tools investigated in this study, namely Jensen's wake model, an actuator disk model, and a Navier-Stokes solver, are described in the third section. The results, in the form of predicted wake velocity profiles and total output power, are presented and discussed in the fourth section, and, finally, a brief summary of our findings and suggestions for future improvements are discussed in the Conclusions.

II. Problem definition

To assess the comparative effectiveness and the limitations of three investigated wake models, the present study was designed such that the "near wake" of an upstream wind turbine would partially overlap the swept area of a downstream wind turbine (Figures 2a & 2b). One of the ultimate objectives of our research is to be able to determine an optimised wind farm turbine layout in terms of number of units versus power losses due to wake interaction. For this reason, the two turbines in the present study are spaced very close together, with just 3.6 rotor diameters between them.

The target turbine is the 5 MW reference wind turbine proposed by Jonkman *et al.* [8] at the National Renewable Energy Laboratory. The turbine, henceforth referred to as the NREL 5 MW turbine, has a rotor diameter of 126 m, and a rated rotor speed of ω = 12.1 rpm at rated wind speed U = 11.4 m/s. This turbine model was selected due to the availability of the turbine's geometrical and operating specifications, making it a very popular model for benchmark studies, with a wide range of experimental and numerical data available for validation purposes. The NREL 5 MW geometry is defined in terms of 17 airfoil profiles with specified radial positions, chord lengths, and local twist angles, as summarised in Table 1.

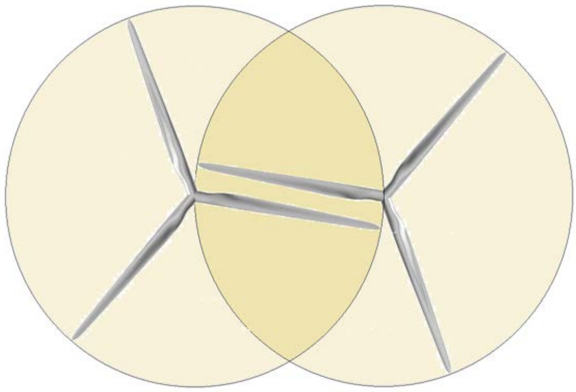

Figure 2a. Partially overlapping swept areas of turbines (front)

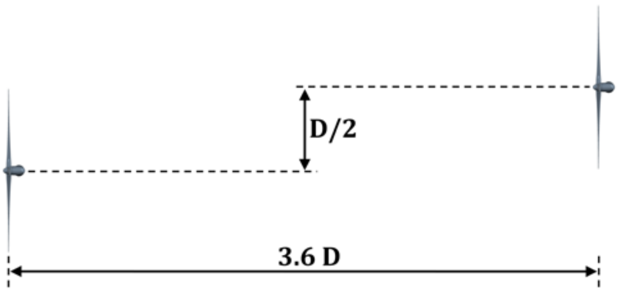

Figure 2b. Two wind turbine array layout (top)

Table 1. NREL 5 MW rotor blade description[8]

Node (-)	RNodes (m)	AeroTwst (°)	DRNodes (m)	Chord (m)	Airfoil Table (-)
1	2.8667	13.308	2.7333	3.542	Cylinder1.dat
2	5.6000	13.308	2.7333	3.854	Cylinder1.dat
3	8.3333	13.308	2.7333	4.167	Cylinder2.dat
4	11.7500	13.308	4.1000	4.557	DU40_A17.dat
5	15.8500	11.480	4.1000	4.652	DU35_A17.dat
6	19.9500	10.162	4.1000	4.458	DU35_A17.dat
7	24.0500	9.011	4.1000	4.249	DU30_A17.dat
8	28.1500	7.795	4.1000	4.007	DU25_A17.dat
9	32.2500	6.544	4.1000	3.748	DU25_A17.dat
10	36.3500	5.361	4.1000	3.502	DU21_A17.dat
11	40.4500	4.188	4.1000	3.256	DU21_A17.dat
12	44.5500	3.125	4.1000	3.010	NACA64_A17.dat
13	48.6500	2.319	4.1000	2.764	NACA64_A17.dat
14	52.7500	1.526	4.1000	2.518	NACA64_A17.dat
15	56.1667	0.863	2.7333	2.313	NACA64_A17.dat
16	58.9000	0.370	2.7333	2.086	NACA64_A17.dat
17	61.6333	0.106	2.7333	1.419	NACA64_A17.dat

The airfoils' vertex data have also been made available, as well as the relationships between several operational parameters with wind speed, such as shown in Figure 3, below. Furthermore, Jonkman's included lift and drag coefficients C_L and C_D have been corrected for rotational stall delay using the Selig and Eggars method.

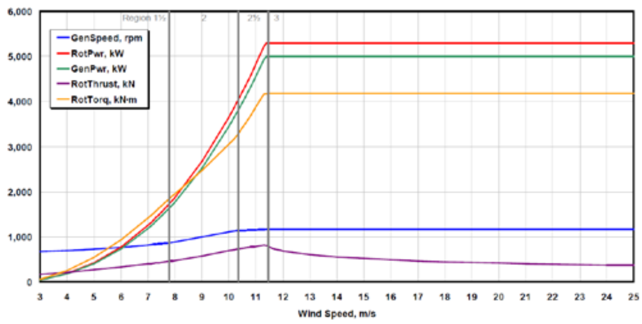

Figure 3. Wind speed curves for NREL 5 MW turbine [8]

III. Numerical models

In this section, we discuss the three numerical models investigated in this study, namely Jensen's empirical wake model, an actuator disk model, and a commercial Navier-Stokes solver.

III a. Jensen's wake model

One of the oldest wake models is that developed by N.O. Jensen in 1983. It is a very simple model, assuming a linearly expanding wake behind a single wind turbine with a velocity deficit that is only dependent of the distance behind the rotor. Figure 4 shows a wake, modelled by Jensen's method, at a horizontal plane through the hub of a GE1.5sl with rotor diameter D. The wake diameter is given by:

$$D_w = D(1 + 2ks) \tag{1}$$

and the velocity in the (fully developed) wake by

$$u = U_\infty \left[1 - \frac{1 - \sqrt{1 - C_t}}{(1 + 2ks)^2}\right] \tag{2}$$

where the relative distance behind the rotor, $s = x/D$ and the Wake Decay Constant is set as $k = 0.04$, which corresponds to the case of low atmospheric turbulence (TI = 8%), often referred to as offshore conditions [9]. The Jensen wake model is employed by Risø DTU's WAsP, GH's WindFarmer, and EMD's WindPRO, to name a few.

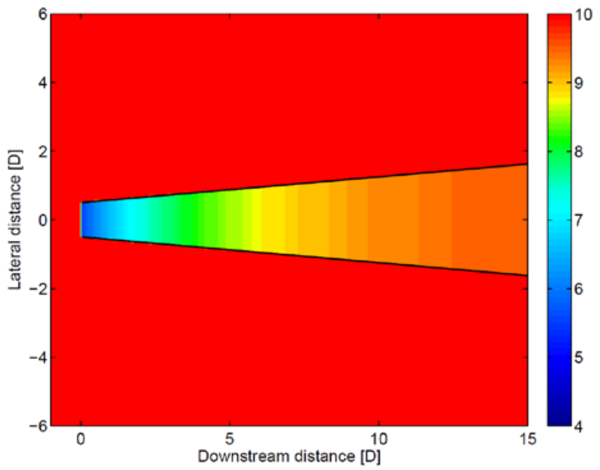

Figure 4. Velocity deficit in the wake behind a wind turbine as predicted by Jensen's model [10]

For the case of multiple wakes, this study employs the 'sum of squares of velocity deficits' wake combination model proposed by Katic [11].

$$\left(1 - \frac{u_j}{U_\infty}\right)^2 = \sum_i \left(1 - \frac{u_{ji}}{u_i}\right)^2 \tag{3}$$

where u_j is the wind speed at turbine j, u_{ji} is the wind speed at turbine j due to the wake of turbine i, and the summation is taken over the i turbines upstream of turbine j.

For the considered case of a partially shadowed downwind turbine, it is necessary to calculate the area of the overlapping regions, as illustrated in Figure 5.

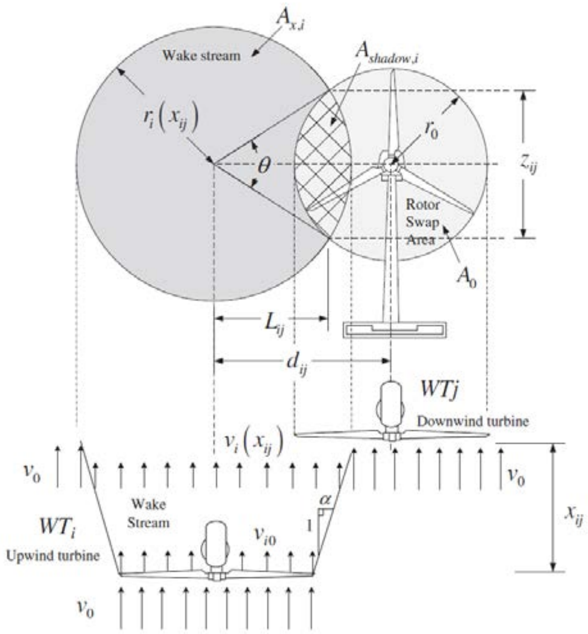

Figure 5. Detailed illustration of partially shadowed downstream turbine, showing all parameters used to calculate A_{shadow} [12]

González-Longatt [12] gives the following equations to calculate the overlapping area A_{shadow}, based on the parameters illustrated in Figure 5, as well as the resulting velocity deficit for a partially shadowed turbine:

$$A_{\text{shadow}} = r_i^2 \cos^{-1}\left(\frac{L_{ij}}{r_i}\right) + r_0^2 \cos^{-1}\left(\frac{d_{ij} - L_{ij}}{r_i}\right) - d_{ij} z_{ij} \tag{4}$$

$$\left(1 - \frac{u_j}{u_i}\right)^2 = \sum_i \left(1 - \frac{u_{ji}}{u_i}\right)^2 \frac{A_{\text{shadow},i}}{A_0} \tag{5}$$

III b. Actuator disk model

This approach makes it possible to investigate the flow field throughout a wind farm without the associated computational expense of resolving the Navier-Stokes equations around the individual wind turbine units. Instead, the effects of the rotor on the flow field are modelled within the so-called actuator disk, which, like the well known blade element momentum (BEM) theory, discretises the rotor into a number of 2D airfoils. The reaction forces of the rotor on the fluid (equal and opposite to the sectional aerodynamic loads on the airfoils, as shown in Figure 6) are calculated by the following equations, and then imposed on RANS [13] or large eddy simulation (LES) [14–16] models of the entire computational domain of a wind farm. The relative inflow velocity for the blade sections are the rotor-coordinate local velocities subtracted from the global ones in the field, as Equation (8) shows.

$$F_n = L\cos\beta - D\sin\beta \ \text{ and } \ F_t = L\sin\beta - D\cos\beta \tag{6}$$

$$L = \tfrac{1}{2}\rho |U_{rel}|^2 C_l c dr \ \text{ and } \ D = \tfrac{1}{2}\rho |U_{rel}|^2 C_d c dr \tag{7}$$

$$\text{where } U_{rel} = u_{global} - u_{rotor} = (u_x + \omega r \sin\psi)\hat{\imath} + (u_y - \omega r \cos\psi)\hat{\jmath} + u_z \hat{k} \tag{8}$$

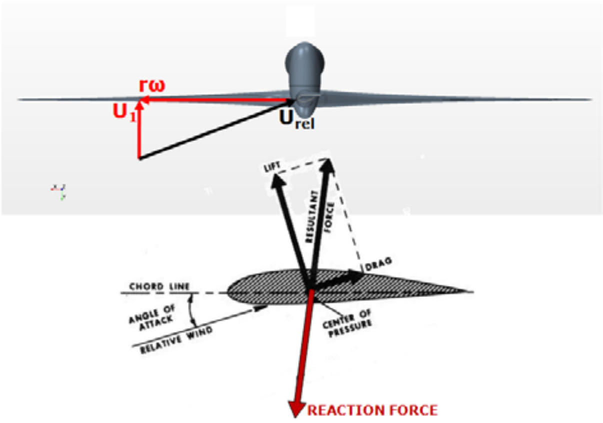

Figure 6. Reaction force on a 2D airfoil element calculated according to local flow field around an operating wind turbine

In this study, we employed the "virtual disk" framework available in the Star-CCM+ commercial software package, which allows the user to define the rotor by means of the airfoils' radial positions, chord lengths, and local twist angles, such as in Table 1, together with the respective 2D airfoil characteristics. By foregoing the resolution of the RANS equations at the rotor surface, the interpolation of rotor forces to the source term f_i of grids, see Figure 7, in RANS Eq. (11) of the global coordinate was done by the following spatially-averaged equation, where b is the number of blades, $\Delta\emptyset$ is the angular distance through which the blade traverses in passing through a blade element and M is the transformation matrix from global to local coordinate systems. The actuator disk model was possible to reduce the number of cells to around 700 000 (see Figure 8). While not as computationally expensive as a full unsteady RANS simulation, this approach may still be considered high fidelity.

$$\begin{bmatrix} f_x \\ f_y \\ f_z \end{bmatrix} = \frac{b\Delta\emptyset}{2\pi}\begin{bmatrix} F_x \\ F_y \\ F_z \end{bmatrix} = -\frac{b\Delta\emptyset}{2\pi}\mathrm{M}^T\begin{bmatrix} F_t \sin\psi \\ F_t \cos\psi \\ F_n \end{bmatrix} \tag{9}$$

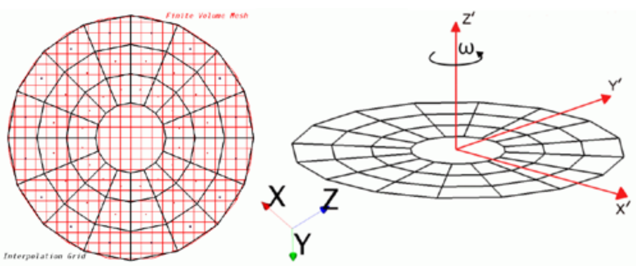

Figure 7. Grid interpolation in actuator disk model

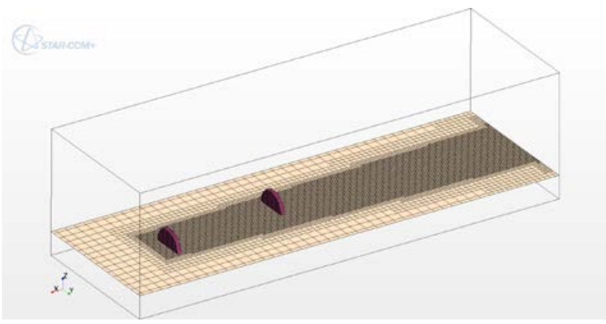

Figure 8. Location of two actuator disks within RANS model

III c. Full RANS simulation

This is the most computationally expensive of the three methods investigated in this study, with a total of 4.5 million cells employed for the simulation of the two turbine array (not to mention a somewhat reduced domain size). For this simulation, we once again used the Star-CCM+ commercial software package. To investigate the transient effects of the rotating blade motion on the downstream turbine, we ran a full, unsteady simulation, with turbulence modelled by the realizable k-ε solver. The modelled domain, showing the locations of the two turbines and the refined mesh near the rotor/hub surfaces, are shown in Figure 9.

$$\frac{\partial u_i}{\partial x_i} = 0 \tag{10}$$

$$\frac{\partial u_i}{\partial t} + \frac{\partial}{\partial x_j}(u_i u_j) = -\frac{1}{\rho}\frac{\partial p}{\partial x_i} + \frac{\partial}{\partial x_j}\left(\nu\left(\frac{\partial u_i}{\partial x_j} + \frac{\partial u_j}{\partial x_i}\right)\right) + \frac{\partial}{\partial x_j}(\acute{u}_i \acute{u}_j) + f_i \tag{11}$$

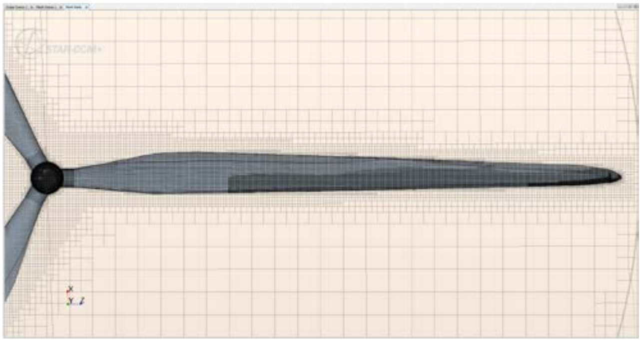

Figure 9. Full RANS computational domain, showing turbine locations and refined mesh near rotor/hub surfaces

IV. Results

The velocity profiles at a distance 2D downstream of the upwind wind turbine WT1 are shown in Figure 10, and the velocity profiles at a distance 2D downstream of the downwind wind turbine WT2 are shown in Figure 11. Despite its simplicity, it is apparent the Jensen wake model is able to provide a reasonable approximation of the velocity deficit downstream of the single wind turbine, while employing the recommended sum of squares approach provides an acceptable approximation of the velocity deficit behind two wind turbines considering partial wake shadowing. Obviously, Jensen's simple model is unable to predict details such as the velocity peak behind the hub, the accelerated flow alongside the wakes, or any other inhomogeneities in the wake. However, since the computation time of this empirical model is negligible, it has found significant favour in the wind farm industry.

The two higher fidelity models offer a far more concise description of the disturbed flow field behind the single and partially shadowed turbines, but at a tremendous increase in computational expense. It is important to note here that the RANS determined velocity profiles presented above are merely a snapshot at one particular instance, carefully selected to highlight the similarities between the wake velocity profiles predicted by the three different approaches. However, due to the close proximity of the two turbines with each other, the downstream turbine is operating in what is typically termed the “near wake”, where the unsteady helical trailing vortices still dominate the wake structure. For this reason, a thorough analysis of the downstream velocity profiles must also consider such unsteady effects. To this end, Figure 12 shows the velocity profile 2D downstream of WT1 at two “time steps” (as represented by the rotor azimuth angle ψ). This figure clearly shows the periodic nature of the fluctuations in the wake, with an almost perfect symmetry seen between the two velocity profiles.

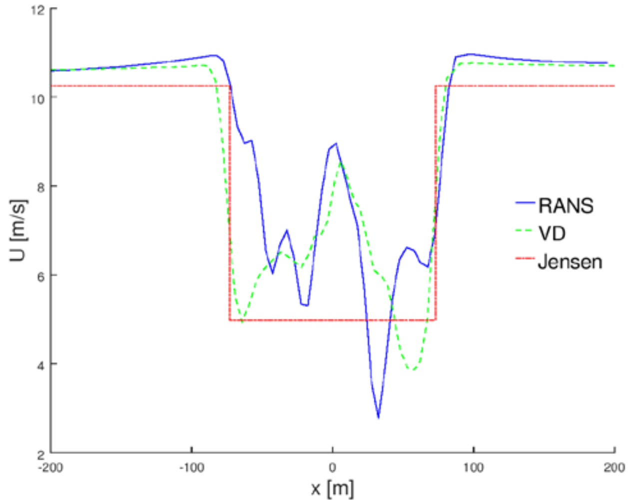

Figure 10. Velocity profiles at WT1 + 2D

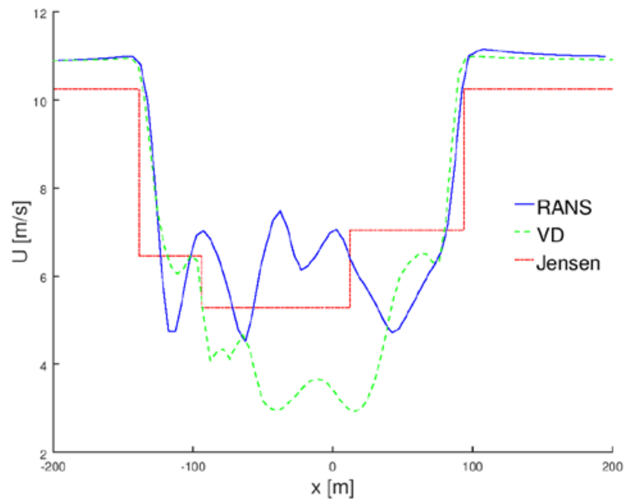

Figure 11. Velocity profiles at WT2 + 2D

Figure 13 shows the effects of the above velocity fluctuations on the wake profile of the downstream turbine WT2. Once again, the two “time steps” are represented by the rotor azimuth angle ψ. This figure clearly shows how the velocity fluctuations have been amplified. In other words, even at a constant inflow velocity, the partially shadowed turbine produces a periodically repeating velocity fluctuation with a 7.4 m/s amplitude at a frequency of 0.6 Hz, which could severely affect the fatigue life of a third turbine located further downstream.

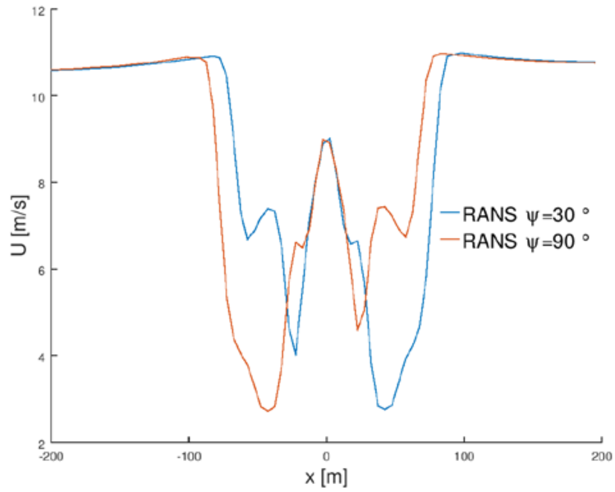

Figure 12. RANS predicted wake velocity profiles at WT1 + 2D at two “time steps” (as represented by rotor azimuth angle ψ)

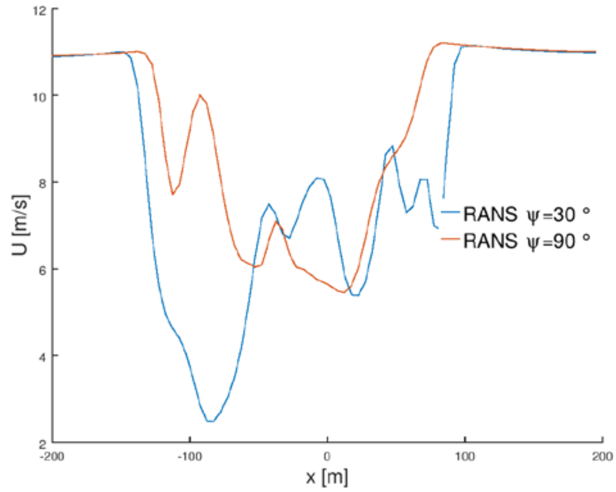

Figure 13. RANS predicted wake velocity profiles at WT2 + 2D at two “time steps” (as represented by rotor azimuth angle ψ).

Finally, the velocity contour plots produced by the two higher fidelity models have been included. Figure 14 (left) shows the velocity contour plots produced by the actuator disk model, while the right shows the velocity contour plots, with rotor surface, produced by the full unsteady RANS model.

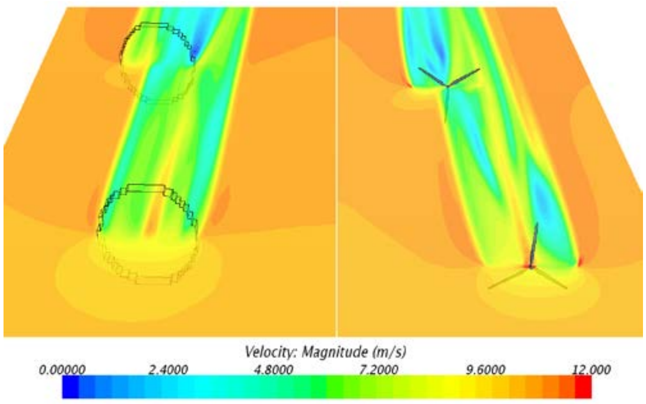

Figure 14. Velocity contour plots in actuator disk model (left) and unsteady RANS simulation (right)

V. Conclusions

This study investigated three numerical tools of varying degrees of fidelity to assess the comparative effectiveness and the limitations of the three approaches in predicting the velocity deficits in the wake behind a single and a partially shadowed wind turbine.

In terms of total power losses, as represented by the steady velocity profiles, the low-fidelity empirical Jensen's model was found to predict the velocity deficits with reasonable accuracy compared with the two higher fidelity approaches.

However, for the purpose of fatigue life assessment, it is imperative that the unsteady effects be considered, and the full unsteady RANS simulation performed in this study showed significant velocity fluctuations are produced in the wake of a partially shadowed turbine.

Further research should be undertaken to study the effects of turbine spacing, to see whether the turbulent mixing that accompanies a greater distance between turbines might reduce the unsteady effects of the shed helical vortices. Moreover, the effectiveness of unsteady "actuator line" models should also be investigated.

References

[1] Global Offshore Wind Speeds Rankings. 4C Offshore. http://www.4coffshore.com (26 January 2017).

[2] Taiwan to invest NT$684 billion to bolster wind energy to 4200 MW by 2025. https://www.evwind.es/2017/05/16/taiwan-to-invest-nt684-billion-to-bolster-wind-energy-to-4200-mw-by-2025/59829 (16 July 2017)

[3] T.Y. Lin, Y. Quéméner, "Extreme Typhoon Loads Effect on the Structural Response of Offshore Meteorological Mast and Wind Turbine", Proceedings of the ASME 2016 35th International Conference on Ocean, Offshore and Arctic Engineering, OMAE2016, 19-24 Jun., 2016, Busan, Korea.

[4] B. Nelson, T.Y. Lin, Y. Quéméner, H.H. Huang, C.Y. Chien, "Extreme Typhoon Loads Effect on the Structural Response of an Offshore Wind Turbine", Proceedings of 7th PAAMES and AMEC2016, 13-14 Oct., 2016, Hong Kong.

[5] FAQ for typhoons. Central Weather Bureau. www.cwb.gov.tw

[6] B. Nelson, T.Y. Lin, Y. Quéméner, H.H. Huang, C.Y. Chien, "Extreme Typhoon Loads Effect on the Structural Response of an Offshore Wind Turbine", Proceedings of 7th PAAMES and AMEC2016, 13-14 Oct., 2016, Hong Kong.

[7] The Wake Effect: Impacting turbine siting agreements. North American Clean Energy. http://www.nacleanenergy.com/articles/15348/the-wake-effect-impacting-turbine-siting-agreements (21 September 2017)

[8] J. Jonkman, S. Butterfield, W. Musial, and G. Scott., Definition of a 5-MW Reference Wind Turbine for Offshore System Development. Technical Report. NREL/TP-500-38060. February 2009.

[9] van Heemst, J.W., Improving the Jensen and Larsen Wake Deficit Models. Using a Free-Wake Vortex Ring Model to Simulate the Near-Wake. MSc Thesis. TUDelft. 2015

[10] Renkema, D.J., Validation of wind turbine wake models. Using wind farm data and wind tunnel measurements. MSc Thesis. TUDelft. 2007

[11] I. Katic, J. Højstrup, and N.O. Jensen. A simple model for cluster effeciency. European Wind Energy Association Conference and Exhibition, 7-9 October 1986, Rome, Italy, 1986.

[12] F. González-Longatt, P. Wall, V. Terzija. Wake effect in wind farm performance: Steady-state and dynamic behavior. Renew. Energy 39(1), 329–338 (2011).

[13] Sørensen, J.N.; Shen, W.Z., Numerical modeling of Wind Turbine Wakes. J Fluids Eng 2002, 124, 393–399

[14] Troldborg, N. Actuator Line Modeling of Wind Turbine Wakes. Ph.D. Thesis, Technical University of Denmark, Lyngby, Denmark, 2008.

[15] Troldborg, N.; Sørensen, J.N.; Mikkelsen, R. Numerical Simulations of Wake Characteristics of a Wind Turbine in Uniform Flow Wind Energy 2010, 13, 86–99.

[16] Lu, H., Porté-Agel, F., "Large-Eddy Simulation of a Very Large Wind Farm in a Stable Atmospheric Boundary Layer," Phys Fluids, 2011, 23, 065101